Research Journal of Environmental Sciences

ISSN 1819-3412

Academic
Journals Inc.

www.academicjournals.com

Research Journal of Environmental Sciences 8 (4): 205-214, 2014
ISSN 1819-3412 / DOI: 10.3923/rjes.2014.205.214

Adsorption of Reactive Blue 19 from Aqueous Solution by Carbon Nano Tubes: Equilibrium, Thermodynamics and Kinetic Studies

[1]Mohammad Rafiee and [2]Mahsa Jahangiri-rad
[1]Department of Environmental Health Engineering, Alborz University of Medical Sciences, Alborz, Iran
[2]Young Researchers and Elites Club, Science and Research Branch, Islamic Azad University, Tehran, Iran

Corresponding Author: Mahsa Jahangiri-rad, Young Researchers and Elites Club, Science and Research Branch, Islamic Azad University, Tehran, Iran

ABSTRACT

Multi-walled and single-walled carbon nanotubes were used as adsorbents for the removal of Reactive Blue 19 textile dye from aqueous solutions. The adsorbents were characterised by scanning and transmission electron microscopy. The effects of pH, shaking time and temperature on adsorption capacity were investigated. The maximum adsorption of dye was observed in the acidic pH region using both adsorbents. The contact time to obtain equilibrium isotherms at 298-323 K was fixed at 2 h for both adsorbents. The equilibrium data were analyzed using three widely applied isotherms: Langmuir, Freundlich and Liu isotherm models. The results revealed that Liu isotherm fit the experimental results well. The maximum sorption capacity for adsorption of the dye occurred at 323 K, attaining values of 450 and 550 mg g^{-1} for MWCNT and SWCNT, respectively. Standard free energy ($\Delta G°$), standard enthalpy ($\Delta H°$) and standard entropy ($\Delta S°$) were calculated by the data obtained from Liu equation at different temperatures. All $\Delta G°$ were negative. The $\Delta h°$ and $\Delta S°$ values were positive; indicating that the reactive blue adsorption was spontaneous and endothermic process.

Key words: Carbon nanotubes, adsorption, reactive blue 19, isotherm models

INTRODUCTION

The release of large amount of dyes into water bodies leads to environmental problems due to their toxic and persistent nature of some of these dyes. It is estimated that about 50% of reactive dyes lost into water ways during manufacturing processes (Crini, 2005). Dyes are usually present in trace quantities in the treated effluents of many industries. The effectiveness of adsorption for dye removal from wastewaters has made it an ideal alternative to other expensive treatment methods (Jahangiri-Rad *et al*., 2013). Various methods have been applied to remove colour from wastewater; among these, carbon nanotube (CNTs) materials have been proposed for the successful removal of dyes from aqueous effluents (Royer *et al*., 2009; Kuo *et al*., 2008). They considered as an attractive alternative for the removal of dye contaminants from aqueous effluents because of their potential as adsorbents due to well defined cylindrical hollow structure, large surface area, high aspect ratios, hydrophobic wall and easily modified surfaces. CNTs have been found to be efficient adsorbents with a capacity that exceeds that of activated carbon (Machado *et al*., 2011). Possibility of product recovery, capability of systems for fully automatic and unattended operation, excellent control, as well as response to process change are some advantages of adsorption process

(Foo and Hameed, 2010). Within this view, multi-walled and single-walled carbon nanotubes were used as adsorbents for the successful removal of Reactive Blue 19 (RB-19) textile dye from aqueous solutions.

MATERIALS AND METHODS

Solutions: Deionised water was used throughout the experiments for solution preparation. The textile dye Reactive Blue 19 (CI 61200; eactiveblue19, also known as Brill. Blue) was furnished by Sigma-Aldrich at 70% purity. The structure of RB 19 is shown in Fig. 1. The dye was used without further purification. A stock solution was prepared by dissolving the RB-19 dye in distilled water to a concentration of 1000 mg L^{-1}. All solutions were prepared using deionized water and reagent grade chemicals working solutions were obtained by diluting the dye stock solution to the required concentrations. To adjust the pH of the solutions, sodium hydroxide or hydrochloric acid solutions were used. The pH of the solutions was measured using a Schott Lab 850 set pH meter.

Adsorbents: Carbon nanotubes were purchased from Iranian Research Institute of Petroleum Industry (RIPI). Carbon nanotubes were subjected to energy dispersive spectrometer for surface distribution of elemental composition and Scanning Electron Microscopy (SEM). Size and morphology of SWCTs were reported by Transmission Electron Microscopy (TEM). The specific surface area of SWCNTs was measured by BET method (Table 1). Pictures of SEM and TEM of selected CNTs are shown in Fig. 2.

Adsorption studies: Batch adsorption experiments were conducted using 100 mL glass bottles with the addition of 30 mg of adsorbents and 50 mL of dye solutions of increasing initial concentration (C_0) from 20 to 200 mg L^{-1}. The solutions were shaken in an illuminated refrigerated incubator shaker (Innova 4340) at ambient temperature (25±2°C). After equilibrating, the solid was separated by centrifugation (3000 rpm) and filtration (0.2 μ). The filtrates were then analysed spectrophotometrically. In the experiments on the effect of temperature, the temperature was held at 298, 303 and 308 K. At the end of equilibrium period, the suspensions were separated for later analysis of the dye concentration. The reproducibility of the measurements was determined from

Table 1: Physical properties of SWCNT and MWCNT adsorbents

Adsorbents	Surface area (m^2 g^{-1})	Total pore volume (cm^3 g^{-1})	Average pore diameter (nm)
SWCNT	355	0.6	5.88
MWCNT	170	0.3	6.87

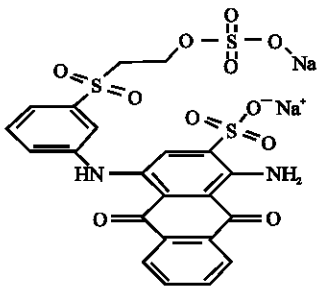

Fig. 1: Structure of RB19

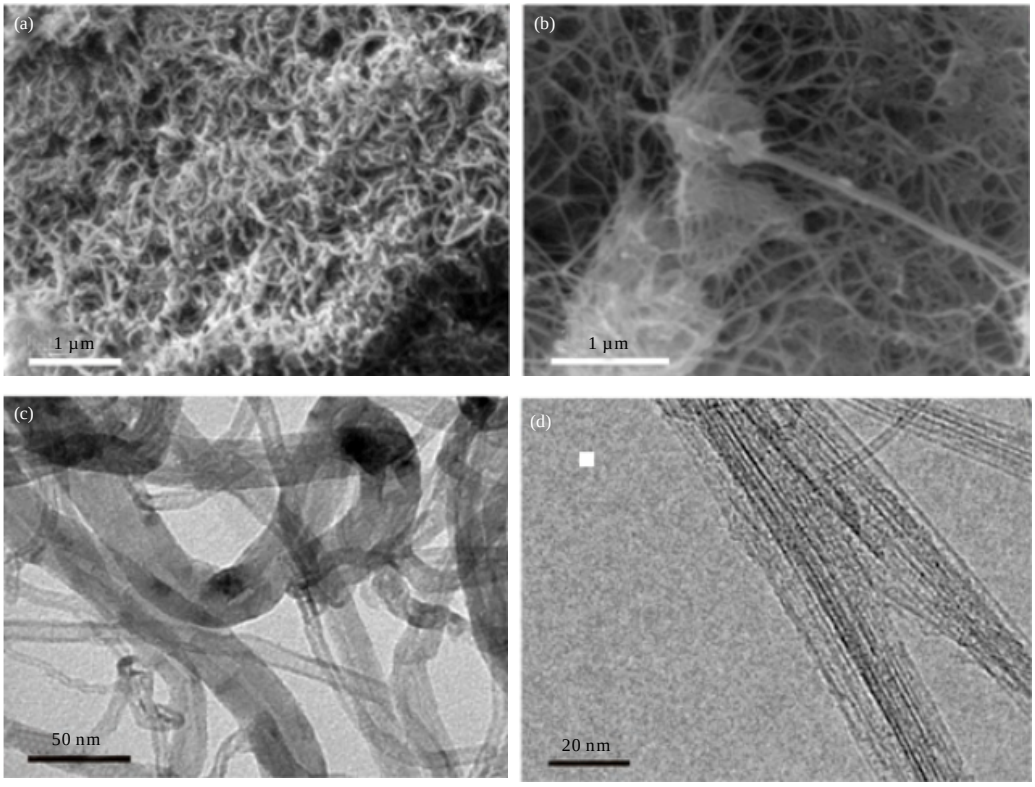

Fig. 2(a-d): SEM and TEM micrographs of (a, c) MWCNT and (b, d) SWCNT

triplicates and average values are reported. The pH of the dye solutions ranged from 2.0-10.0. Subsequently, the final concentrations of the dye which remained in the solution were determined by visible spectrophotometry using a UV-VIS spectrophotometer. Absorbance measurements were made at the maximum wavelength of RB19 dye at 590 nm. The amount of dye taken up and the percentage of removal of the dye by the adsorbent were calculated by applying Eq. 1 and 2, respectively:

$$q_e = \frac{(C_0 - C_e).V}{m} \quad (1)$$

$$\text{Removal}\ (\%) = \left(\frac{C_0 - C_e}{C_0}\right) \times 100 \quad (2)$$

where, q is the amount of dye taken up by the adsorbent (mg g^{-1}), C_o is the initial dye concentration put in contact with the adsorbent (mg L^{-1}), C_e is the dye concentration (mg L^{-1}) after the batch adsorption procedure, m is adsorbent mass (g) and V is the volume of the dye solution (L).

Equilibrium models and its statistical evaluation: The equilibrium of adsorption was evaluated using the Langmuir, Freundlich and Liu isotherm models (Geyikci, 2013). The isotherm equations are given in Table 1.

The validity of models was determined by calculating the standard deviation as follows (Eq. 3):

$$S.D. = \sqrt{\frac{\sum\left[\left(q_{exp} - q_{cal}\right)\right]/q_{exp}}{n-1}} \quad (3)$$

where, the exp and cal are the experimental and calculated data and n is the number of data points.

RESULTS AND DISCUSSION

Characterisation of the adsorbents: The properties of the MWCNT and SWCNT adsorbents are presented in Table 1. Based on these results, it would be expected that SWCNT would present a higher sorption capacity than MWCNT, since the specific surface area and total pore volume of SWCNT were higher than for MWCNT, respectively. It was also observed that MWCNT presented a higher average pore diameter compared to SWCNT. This higher textural parameter could be attributed to the aggregated pores formed in MWCNT.

TEM and SEM images (Fig. 2) show the morphological structure of the MWCNT (Fig. 2a, c) and SWCNT (Fig. 2b, d) adsorbents. The SEM image in Fig. 2a shows entanglement of MWCNT and Fig. 2b shows SWCNT in thin bundles. The outer diameters of the MWCNT (Fig. 2c) and SWCNT (Fig. 2d) are in the range of 5-40 and 1-2 nm, respectively.

Effects of pH on adsorption: One of the most important factors in adsorption studies is the effect of acidity on the medium (Jacques *et al*., 2007). Different species may present divergent ranges of suitable pH depending on which adsorbent is used. The effect of pH on the uptake of dye was monitored in the pH range 3-10 (Fig. 3). It is clear that the pH plays a key role in affecting the adsorption rate of RB 19. The adsorption of RB19 was more favored in acid solution. For both adsorbents, the percentage of dye removal decreased from pH 3.0 up to 10.0. For pH values lower than pH_{pzc} (zero point charge), the adsorbent presents a positive surface charge. SWCNT and MWCNT exhibited strong adsorption of RB19 when pH was between 3 and 6 which can be

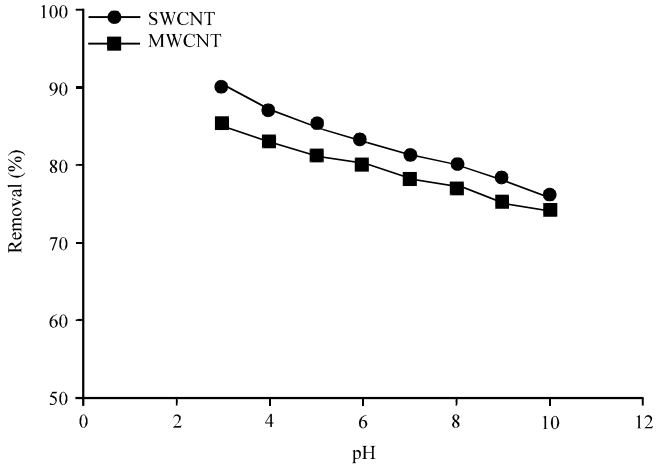

Fig. 3: Effect of pH on the adsorption of RB 19 dye on MWCNT and SWCNT

Table 2: Isotherm models

Isotherm model	Equation	
Langmuir	$q_e = \frac{Q_{max}.K_L.C_e}{1+K_L.C_e}$	(3)
Freundlich	$q_e = K_F.C_e^{1/n_F}$	(4)
Liu	$q_e = \frac{Q_{max}.(K_g.C_e)^{n_L}}{1+(K_g.C_e)^{n_L}}$	(5)

Table 3: Liu isotherm parameters for RB19 adsorption, using MWCNT and SWCNT as adsorbents

	SWCNT			MWCNT		
Parameters	298 K	303 K	323 K	298 K	303 K	323 K
Q_{max} (mg g^{-1})	487.6	518.6	550.7	442.0	447.4	450
K_g (L mg^{-1})	0.82	0.933	2.00	0.458	0.602	0.701
n_L	0.4303	0.2008	0.55	0.721	0.509	0.4821
R^2	0.9997	0.9999	0.9997	0.9998	0.9999	0.9996
S.D	8.5	7.0	8.5	8.6	6.8	9.0

explained by the electrostatic attraction between the positive charged of selected CNTs and RB19. The dissolved RB19 dye is negatively charged in aqueous solution, because it possesses three sulphonate groups. The adsorption of this dye takes place when the adsorbents present a positive surface charge. When the pH value is much lower than pH_{pzc}, the surface of the adsorbent becomes more positive (Hlavay and Polyak, 2005). This behaviour explains the high adsorption capacity of both adsorbents for RB19 dye at pH 3.0. In order to continue the adsorption studies, the initial pH was fixed at 3.0.

Equilibrium studies: An adsorption isotherm describes the relationship between the amount of adsorbate taken up by the adsorbent (q_e) and the adsorbate concentration remaining in the solution after the system has attained equilibrium (C_e). In this study, the Langmuir, Freundlich and Liu isotherm models were tested. The isotherm equations are given in Table 2. The isotherms of adsorption were carried out from 298 to 323 K. The adsorption isotherms of RB19 on to SWCNT and MWCNT are shown in Fig. 4. As can be seen with the increasing mass ratio of CNTs, the amount of adsorbed dye increased significantly. The Langmuir isotherm model is based on the fact that adsorbates are chemically adsorbed at a fixed number of well-defined sites; each site can only take one adsorbate species; all sites are energetically similar; there are no interactions between the adsorbate species (Lv, 2007). The Freundlich isotherm model is an empirical relationship which assumes that the ratio of the amount of solute adsorbed onto a given mass of adsorbate to the concentration of the solute in solution is not constant at different solution concentrations. In other words, different sites with distinct adsorption energies are involved (Biswas *et al*., 2007). The Liu isotherm model is a combination of the Langmuir and Freundlich isotherm models; therefore, the monolayer assumption of Langmuir model is eliminated and the infinite adsorption assumption that originates from the Freundlich model is also overruled. The Liu model predicts that the active sites of the adsorbent cannot have the same energy. Therefore, the adsorbent may have active sites preferred by the adsorbate molecules for occupation (Prola *et al*., 2013a); Considering various functional groups on the carbon nanotubes our results shows that the active sites of the carbon nanotubes will not have the same energy. Due to the lower S.D and higher R^2 values calculated from Liu isotherm this model fitted the experimental data well (Table 3). The maximum amounts

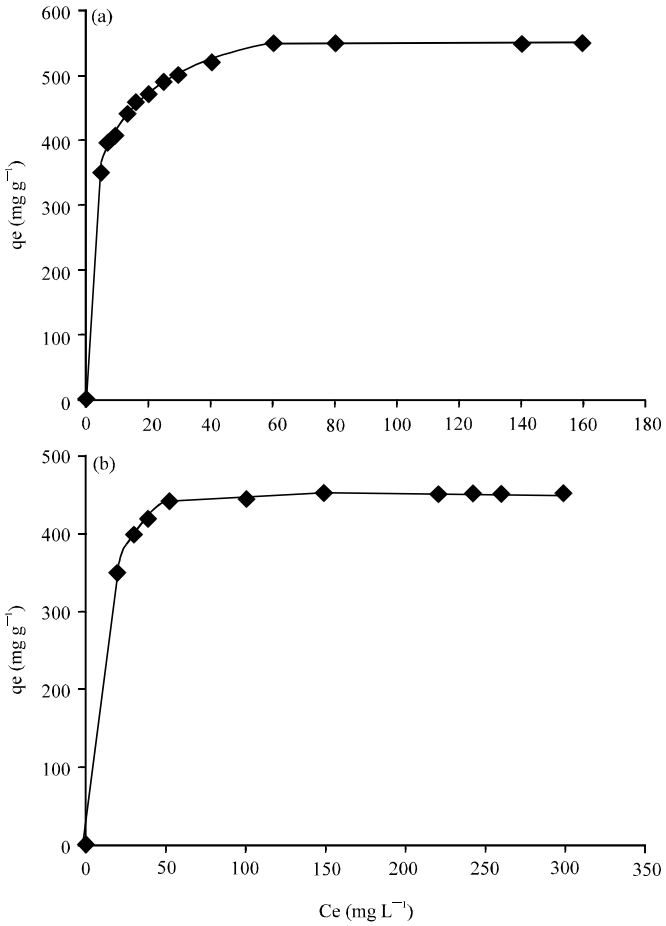

Fig. 4(a-b): Adsorption isotherm of RB19 onto (a) SWCNT and (b) MWCNT

Table 4: Some previously reported adsorption capacities of different adsorbents for RB19

Adsorbent	q_e (mg g^{-1})	References
Modified bentonite	130	Gok *et al.* (2010)
Wheat bran	117.6	Cicek *et al.* (2007)
Seawater neutralised bauxite refinery residue	250	De Souza *et al.* (2013)
Carbon nanotubes	450-550	This study

of RB19 uptake were 450 and 550 mg g^{-1} for MWCNT and SWCNT at 323 K, respectively. Previously some researchers investigated several adsorbents for the removal of reactive dyes from aqueous solutions. By comparing the data obtained in the previous works and results obtained in this study (Table 4) on adsorption capacities, it can be indicated that these adsorbents are very good for RB19 dye removal from aqueous solutions. It should be highlighted that the maximum amount of RB19 dye adsorbed on SWCNT was higher than the value obtained on MWCNT due to the textural characteristics of MWCNT.

Effect of contact time: The adsorption of dye was investigated as a function of contact time with an initial solution pH of 3. It is clear that RB19 removal increased with time for both adsorbents

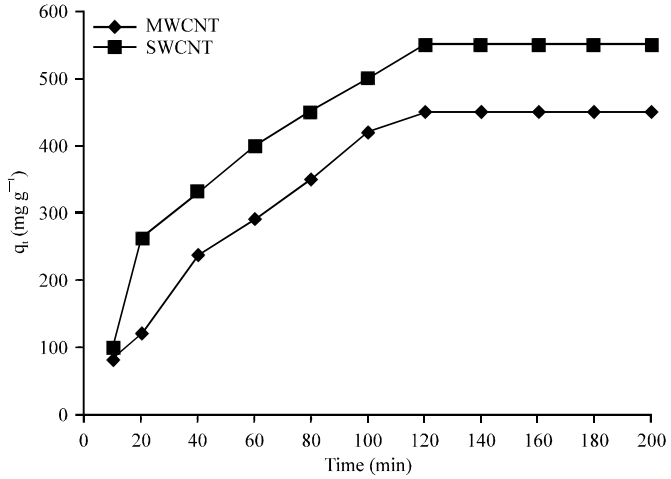

Fig. 5: Effect of contact time on the adsorption of RB19 dye on CNTs

(Fig. 5). As shown dye uptake was rapid in the beginning and gradually reached a plateau. Maximum dye uptake was observed within the first 2 h and then after RB19 removal was not significant.

Thermodynamic analysis: In adsorption processes the temperature plays an important role in determining thermodynamic dependency. The nature and thermodynamic feasibility of the sorption process were analyzed by standard free energy (ΔG°), standard enthalpy (ΔH°) and standard entropy (ΔS°) using the following equations (Eq. 4, 5) (Moreira *et al.*, 2001):

$$\Delta G^\circ = -RTLn(K_L) \tag{4}$$

$$Ln(K_L) = \frac{\Delta S^\circ}{R} - \frac{\Delta H^\circ}{RT} \tag{5}$$

where, K_L is the Langmuir constant (L mol^{-1}), R is the gas constant and T is the temperature (K). On the basis of Eq. 4, the values of Gibb's free energy were calculated as -30,-31.5 and -35 kJ mol^{-1} at temperatures of 298, 303 and 323 K for SWCNT, respectively. For MWCNT these values obtained as -28.8, -30 and -31.6 at temperatures of 298, 303 and 323 K, respectively. The negative values of ΔG° suggest feasibility of the process, while increase in values of ΔG° indicates that the adsorption process becomes more favorable at higher temperatures. Enthalpy changes (ΔH°) for SWCNT and MWCNT were 25.33 and 20.98 J mol^{-1} indicate that the adsorption is an endothermic processes. The positive values of ΔS° obtained by Eq. 5 were 201 and 175 J mol K^{-1}, respectively; suggest the affinity of the adsorbents for RB19. A study demonstrated the same results and they concluded that positive values of ΔS° is a confirmation of high preference dye molecules on the adsorbents and suggested the possibility of some structural changes or readjustments in the dye-carbon adsorption complex (Prola *et al.*, 2013b).

Design of batch sorption from isotherm data: A schematic diagram of a batch sorption process is shown in Fig. 6. As shown in this figure, the RB19 with the initial volume (V) and

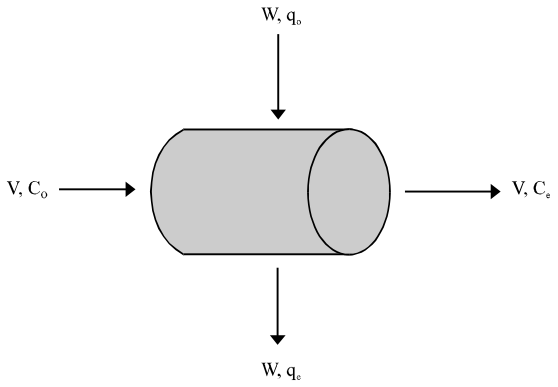

Fig. 6: Batch sorption process

concentration (C_0) reached equilibrium and dye concentration reduced to C_e. In batch adsorption process selected mass (W) of SWCNT or MWCNT was added to the solution and the amount of dye adsorbed changed from q_0 to q_e.

The mass balance can be calculated as (Eq. 6):

$$V\,(C_0-C_e) = W\,(q_o-q_e) \tag{6}$$

Data obtaines from our results fitted well Liu isotherm. Therefore, the Eq. 6 can be rearenged as (Eq. 7):

$$\frac{W}{V} = \frac{C_o - C_e}{q_e} = \frac{(C_o - C_e)\left(1+\left(K_g.C_e\right)^{nl}\right)}{Q_{max}.\left(K_g.C_e\right)^{nl}} \tag{7}$$

Intra-particle diffusion kinetic analysis: In order to investigate the mechanism of the adsorption of RB19 onto CNTs, the experimental data were analyzed against the intraparticle diffusion model to identify the mechanism involved in the sorption process. Intra-particle diffusion model, expressed as (Weber and Morris, 1963):

$$qt = k_i t^{1/2} + C \tag{8}$$

where, C is the intercept and K_i is the intra-particle diffusion rate constant (mg g^{-1} $min^{1/2}$). The three consecutive steps in the sorption of a sorbate by a porous sorbent are: (1) Mass transfer across the external boundary layer film of liquid surrounding the outside of the particle, (2) Adsorption at a site on the surface (internal or external) and the energy will depend on the binding process (physical or chemical), this step is often assumed to be extremely rapid, (3) Diffusion of the adsorbate molecules to an adsorption site either by a pore diffusion process through the liquid filled pores or by a solid surface diffusion mechanism (Cheung *et al*., 2007). Figure 7 shows the plot of q_t vs. $t^{1/2}$. As shown the data exhibit multi linear plots, indicating that the process is governed by two or more steps (phase I and phase II). Phase I shows external mass transfer while phase II exhibits intraparticle or pore diffusion (Aguilar-Carrillo *et al*., 2006).

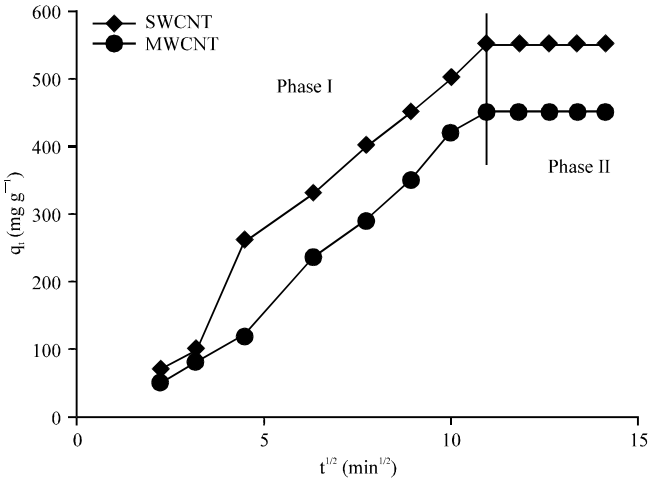

Fig. 7: Intraparticle diffusion kinetics of RB19 onto CNTs

CONCLUSION

Multi-Walled Carbon Nanotubes (MWCNT) and Single-Walled Carbon Nanotubes (SWCNT) were good adsorbents for removing Reactive Blue 19 textile dye from aqueous solutions. The sorption of dye on CNTs was found to be pH dependent with maximum dye removal occurring at pH 3. The maximum adsorption capacity of SWCNT and MWCNT were 550 and 450 mg g^{-1} , respectively. The equilibrium isotherm of the RB-19 dye was obtained and these data were best fit to the Liu isotherm model. Thermodynamic analyses indicate that the sorption of RB19 onto CNTs was endothermic and spontaneous.

ACKNOWLEDGMENTS

The authors are grateful to thank environmental labarotary staff for their collaboration in this research.

REFERENCES

Aguilar-Carrillo, J., F. Garrido, L. Barrios and M.T. Garcia-Gonzalez, 2006. Sorption of As, Cd and Tl as influenced by industrial by-products applied to an acidic soil: Equilibrium and kinetic experiments. Chemosphere, 65: 2377-2387.

Biswas, K., S.K. Saha and U.C. Ghosh, 2007. Adsorption of fluoride from aqueous solution by a synthetic iron (III)-aluminum (III) mixed oxide. Ind. Eng. Chem. Res., 46: 5346-5356.

Cheung, W.H., Y.S. Szeto and G. McKay, 2007. Intraparticle diffusion processes during acid dye adsorption onto chitosan. Bioresour. Technol., 98: 2897-2904.

Cicek, F., D. Ozer, A. Ozer and A. Ozer, 2007. Low cost removal of reactive dyes using wheat bran. J. Hazard. Mater., 146: 408-416.

Crini, G., 2005. Recent developments in polysaccharide-based materials used as adsorbents in wastewater treatment. Prog. Polym. Sci., 30: 38-70.

De Souza, K.C., M.L.P. Antunes, S.J. Couperthwaite, F.T. da Conceicao, T.R. de Barros and R. Frost, 2013. Adsorption of reactive dye on seawater-neutralised bauxite refinery residue. J. Colloid Interface Sci., 396: 210-214.

Foo, K.Y. and B.H. Hameed, 2010. Insights into the modeling of adsorption isotherm systems. Chem. Eng. J., 156: 2-10.

Geyikci, F., 2013. Adsorption of acid blue 161 (AB 161) dye from water by multi-walled carbon nanotubes. Fullerenes Nanotubes Carbon Nanostruct., 21: 579-593.

Gok, O., A.S. Ozcan and A. Ozcan, 2010. Adsorption behavior of a textile dye of Reactive Blue 19 from aqueous solutions onto modified bentonite. Applied Surf. Sci., 256: 5439-5443.

Hlavay, J. and K. Polyak, 2005. Determination of surface properties of iron hydroxide-coated alumina adsorbent prepared for removal of arsenic from drinking water. J. Colloid Interface Sci., 284: 71-77.

Jacques, R.A., E.C. Lima, S.L. Dias, A.C. Mazzocato and F.A. Pavan, 2007. Yellow passion-fruit shell as biosorbent to remove Cr (III) and Pb (II) from aqueous solution. Separat. Purif. Technol., 57: 193-198.

Jahangiri-Rad, M., K. Nadafi, A. Mesdaghinia, R. Nabizadeh, M. Younesian and M. Rafiee, 2013. Sequential study on reactive blue 29 dye removal from aqueous solution by peroxy acid and single wall carbon nanotubes: Experiment and theory. Iran. J. Environ. Health Sci. Eng., Vol. 10 10.1186/1735-2746-10-5

Kuo, C.Y., C.H. Wu and J.Y. Wu, 2008. Adsorption of direct dyes from aqueous solutions by carbon nanotubes: Determination of equilibrium, kinetics and thermodynamics parameters. J. Colloid Interface Sci., 327: 308-315.

Lv, L., 2007. Defluoridation of drinking water by calcined MgAl-CO_3 layered double hydroxides. Desalination, 208: 125-133.

Machado, F.M., C.P. Bergmann, T.H. Fernandes, E.C. Lima, B. Royer, T. Calvete and S.B. Fagan, 2011. Adsorption of Reactive Red M-2BE dye from water solutions by multi-walled carbon nanotubes and activated carbon. J. Hazard. Mater., 192: 1122-1131.

Moreira, R.F.P.M., J.L. Soares, H.J. Jose and A.E. Rodrigues, 2001. The removal of reactive dyes using high-ash char. Braz. J. Chem. Eng., 18: 327-336.

Prola, L.D.T., E. Acayanka, E.C. Lima, C.S. Umpierres and J.C. Vaghetti *et al.*, 2013a. Comparison of *Jatropha curcas* shells in natural form and treated by non-thermal plasma as biosorbents for removal of Reactive Red 120 textile dye from aqueous solution. Ind. Crops Prod., 46: 328-340.

Prola, L.D.T., F.M. Machado, C.P. Bergmann, F.E. de Souza and C.R. Gally *et al.*, 2013b. Adsorption of Direct Blue 53 dye from aqueous solutions by multi-walled carbon nanotubes and activated carbon. J. Environ. Manage., 130: 166-175.

Royer, B., N.F. Cardoso, E.C. Lima, V.S. Ruiz, T.R. Macedo and C. Airoldi, 2009. Organofunctionalized kenyaite for dye removal from aqueous solution. J. Colloid Interface Sci., 336: 398-405.

Weber, W.J. and J.C. Morris, 1963. Kinetics of adsorption on carbon from solution. J. Sanit. Eng. Div., 89: 31-60.